Orientation change detection and orientation pooling in space and time performed by two subpopulations of neurons in V2

Weill Cornell Medical College

Anita M. Schmid, Jonathan D. Victor

Department of Neurology & Neuroscience, Weill Cornell Medical College, New York, NY

INTRODUCTION

In natural images, some boundaries are defined by luminance differences; others are defined by texture differences. Most neurons in primary visual cortex (V1) are well-driven by luminance boundaries at the appropriate orientation[1-2]. Boundaries defined by differences in texture, however, are more effective stimuli for neurons in the secondary visual cortex (V2)[3-9]. Since the larger receptive fields of V2 are produced by combining the output of V1 neurons[10-12], the extraction of texture boundaries by V2 receptive fields must involve computations on its V1 inputs across space. These computations must accomplish a specific goal – extraction of texture boundaries – while preserving the luminance-boundary information already extracted by V1.

How do V2 neurons combine V1 receptive fields?

METHODS

- Grid of rectangles containing sinusoidal gratings (4 x 5 or 6 x 6)
- Preferred orientation or orthogonal orientation
- Grid aligned with receptive field, covering surround
- Pseudo-random sequences (m-sequences)
- Frame rates of 20 or 40 ms (results shown for 20 ms)
- Measuring first-order as well as second-order responses
- Reverse correlation
- Anesthetized and paralyzed macaques
- Extracellular single unit recordings using tetrodes

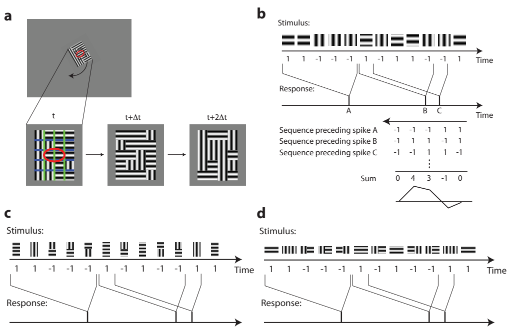

Figure 1. Orientation discontinuity stimulus and kernel computation.
(a) Stimulus setup. A 4 x 5 grid of rectangular regions covered the classical (red ellipse) and non-classical receptive field. The stimulus was aligned with the preferred orientation of the receptive field. Each region contained a static sinusoidal grating with either the preferred or the orthogonal, non-preferred orientation. The orientation in each region changed every 20 milliseconds. Blue and green lines show the region boundaries parallel (blue) and orthogonal (green) to the receptive field; these lines were not part of the stimulus. (b) Computation of a first-order kernel. For each region in the stimulus, the neuron's spike response was cross-correlated with the stimulus sequence, coded as +1 for the preferred orientation and -1 for the orthogonal orientation. Note that spatial phase is randomized. (c) Computation of the spatial second-order kernel across boundaries parallel to the receptive field. The response is correlated with the product of the values of the stimulus in the two neighboring regions: 1 if the grating orientation in the two regions is equal and -1 if they are different. (d) Analogous computation of the spatial second-order kernel across boundaries orthogonal to the receptive field.

RESULTS

First-order kernels:
Responses to the orientation of gratings in individual regions.

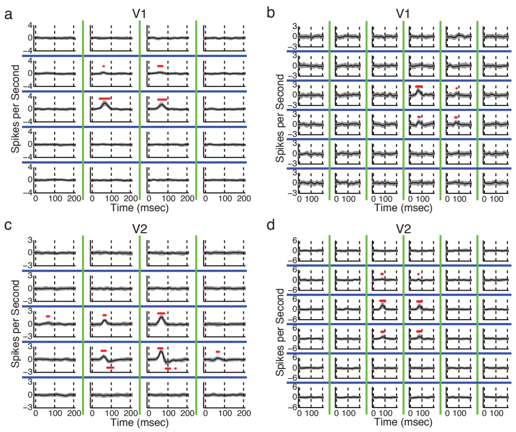

Figure 2. First-order response kernels.
(a) First-order response kernels of a neuron in V1. The check size of the stimulus was 0.4 x 0.75 degrees of visual angle. The response kernel is plotted for each rectangular region in the stimulus; blue and green lines correspond to subdivisions of the stimulus (compare Figure 1a). The mean response kernel (of 32 repetitions) is plotted in black and the jackknife estimate of the standard deviation in gray. Asterisks mark timepoints at which the response is significantly different from zero (two-tailed t-test, α = 0.01, corrected for multiple comparisons). Dashed vertical lines show the timepoints 0, 100 and 200 milliseconds. (b) First-order response kernels of another V1 neuron. The check size of the stimulus was 0.4 x 0.4 degrees of visual angle. (c) First-order response kernels of a V2 neuron. The check size of the stimulus was 0.6 x 0.75 degrees of visual angle. (d) First-order response kernels of a V2 neuron. The check size of the stimulus was 0.4 x 0.2 degrees of visual angle.

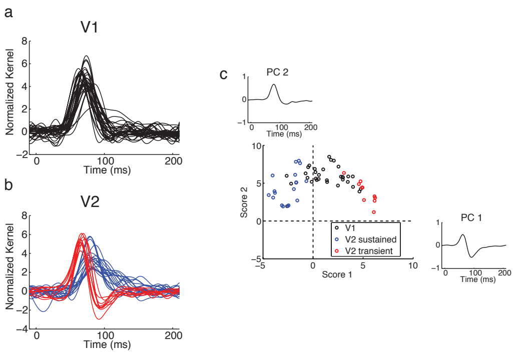

Figure 3. Population summary of first-order kernels.
(a) Normalized first-order response kernels of V1 neurons. (b) Normalized first-order response kernels of V2 neurons, monophasic responses are colored blue and biphasic responses red. (c) First and second scores of PCA decomposition of all normalized first-order kernels. The corresponding principal components are plotted in insets along the corresponding axes. V1 kernels are colored in black; biphasic V2 kernels (first score larger than 0) in red; monophasic V2 kernels (first score smaller than 0) in blue.

Second-order kernels:
Responses to combinations of gratings in neighboring regions.

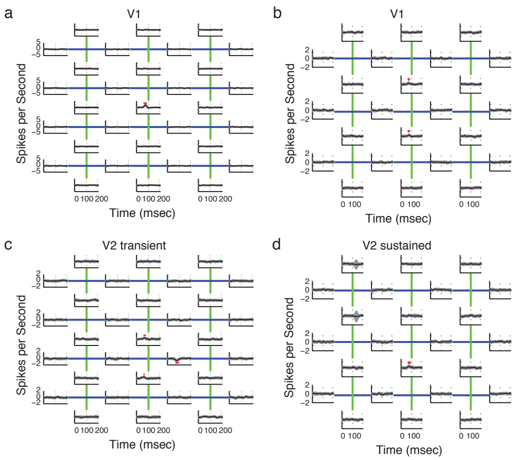

Figure 4. Spatial second-order response kernels.
(a) Second-order response kernels of a neuron in V1. The check size of the stimulus was 0.4 x 75 degrees of visual angle. Colored lines depict the boundaries between the 20 regions, the green lines stand for boundaries orthogonal to the receptive fields preferred orientation and blue lines for those parallel. The response kernels are plotted on the line corresponding to the boundary between the corresponding two neighboring regions. The mean response kernel (of 32 repetitions) is plotted in black and the jackknife estimate of the standard deviation in gray. Asterisks mark timepoints at which the response is significantly different from zero (two-tailed t-test, α = 0.01, corrected for multiple comparisons). Dashed vertical lines show the timepoints 0, 100 and 200 milliseconds. (b) Second-order response kernels of another neuron in V1. The layout was 6 x 6 and the check size of the stimulus 0.4 x 0.4 degrees of visual angle. Only kernels for a 4 x 4 subregion centered on the receptive field are shown. (c) Second-order response kernels of a 'transient' neuron in V2 (same as in Figure 2c). (d) Second-order response kernels of a 'sustained' neuron in V2. The layout was 6 x 6 and the check size of the stimulus 0.4 x 0.2 degrees of visual angle. Only kernels for a 4 x 4 subregion centered on the receptive field are shown.

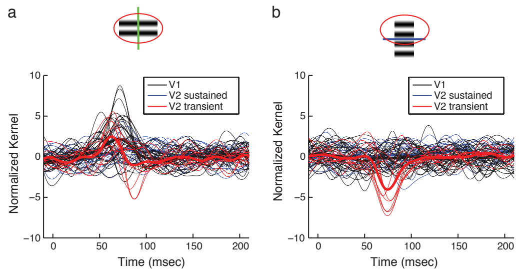

Figure 5. Population summary of spatial second-order response kernels.
(a) Normalized second-order response kernels to boundaries orthogonal to the receptive field (corresponding to green lines in Figure 1a). The thick lines show the population average for V1 neurons in black, transient V2 neurons in red and sustained V2 neurons in blue. (b) Normalized second-order responses to boundaries parallel to the receptive field (corresponding to blue lines in Figure 1a).

SUMMARY

V1 neurons:

Consistent timing across the population

- Monophasic responses to orientation signal in individual regions
- Monophasic "positive" responses to combinations of orientations in neighboring patches. This yields larger responses to continuous orientation than to discontinuities.

V2 neurons:

Two distinct patterns of responses

'Transient V2 neurons':

- Biphasic responses to orientation signal in individual regions. This means that the optimal stimulus within a patch is the non-preferred orientation followed by the preferred orientation and yields larger responses to changing orientation than to static orientation over time.
- Biphasic or monophasic "negative" responses to combinations of orientations in neighboring patches. This yields larger responses to discontinuities than to continuous orientation.

'Sustained V2 neurons':

- Monophasic responses to orientation signals in individual regions, with a broader peak than the V1 responses.
- No measurable nonlinear spatial interaction.

CONCLUSIONS

This study shows, firstly, how non-linear as well as linear responses of V2 neurons differ from V1 responses. Secondly, we identified two different classes of orientation selective V2 neurons. The transient V2 neurons differentiate the V1 input in space and time and therefore respond well to changes in orientation. Sustained V2 neurons pool the V1 input and respond better to constant orientation signals.

References:

1. Hubel DH, Wiesel TN (1959), J Physiol 148:574-591.
2. Hubel DH, Wiesel TN (1968), J Physiol 195:215-243.
3. von der Heydt R, Peterhans E, Baumgartner G (1984), Science 224:1260-1262.
4. von der Heydt R, Peterhans E (1989), J Neurosci 9:1731-1748.
5. Grosof DH, Shapley RM, Hawken MJ (1993), Nature 365:550-552.
6. Leventhal AG, Wang Y, Schmolesky MT, Zhou Y (1998), Vis Neurosci 15:1107-1118.
7. Marcar VL, Raiguel SE, Xiao D, Orban GA (2000), J Neurophysiol 84:2786-2798.
8. von der Heydt R, Zhou H, Friedman HS (2000), Vision Res 40:1955-1967.
9. Song Y, Baker CL, Jr. (2007), Vis Neurosci 24:65-77.
10. Foster KH, Gaska JP, Nagler M, Pollen DA (1985), J Physiol 365:331-363.
11. Levitt JB, Kiper DC, Movshon JA (1994), J Neurophysiol 71:2517-2542.
12. Smith MA, Kohn A, Movshon JA (2007), J Vis 7:5.

Acknowledgment:
This study was supported by grant NIH EY09314.